

Learning Visual-Audio Representations for Voice-Controlled Robots

Peixin Chang, Shuijing Liu, and Katherine Driggs-Campbell

Abstract—Inspired by sensorimotor theory, we propose a novel pipeline for task-oriented voice-controlled robots. Previous method relies on a large amount of labels as well as task-specific reward functions. Not only can such an approach hardly be improved after the deployment, but also has limited generalization across robotic platforms and tasks. To address these problems, we learn a visual-audio representation (VAR) that associates images and sound commands with minimal supervision. Using this representation, we generate an intrinsic reward function to learn robot policies with reinforcement learning, which eliminates the laborious reward engineering process. We demonstrate our approach on various robotic platforms, where the robots hear an audio command, identify the associated target object, and perform precise control to fulfill the sound command. We show that our method outperforms previous work across various sound types and robotic tasks even with fewer amount of labels. We successfully deploy the policy learned in a simulator to a real Kinova Gen3. We also demonstrate that our VAR and the intrinsic reward function allows the robot to improve itself using only a small amount of labeled data collected in the real world.

I. INTRODUCTION

As robots begin to enter people’s daily lives, there is an increasing need for intuitive ways that allow non-experts to interact and communicate with robots. Spoken language is a natural choice for communication, leading to a wealth of research in task-oriented voice-controlled robots [1]. Conventional pipelines for task-oriented voice-controlled robots consist of independent modules for automatic speech recognition (ASR), natural language understanding (NLU), symbol grounding, and motion planning, as shown in Fig. 2a. These pipelines suffer from intermediate and cascading errors between different modules and the difficulties in relating language to the physical entities it refers to [2]. To address these challenges, several approaches attempt to jointly optimize some of the independent modules [3], [4]. However, these approaches only consider part of the pipeline and cannot solve voice-controlled tasks alone.

The first end-to-end model for task-oriented voice-controlled robots and the concept of Robot Sound Interpretation (RSI) is proposed in [5]. RSI considers typical tasks for voice-controlled robots, where an audio command serves as a goal, as illustrated in Fig. 1. After hearing a sound command, the robot must identify the goal of the commander (intent), draw the correspondence between the raw visual and audio inputs, and develop a policy to approach the

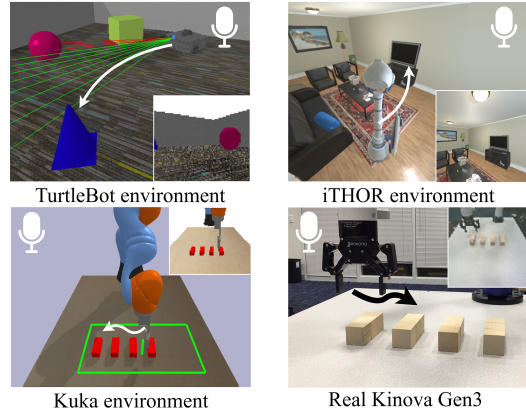


Fig. 1: **Illustration of our robotic tasks.** The robots must approach a target mentioned by a sound command to finish a task. Windowed image shows the robot camera view. The green and red lines are for illustration purposes and is invisible to the robot. *Top left:* The TurtleBot searches for then navigates to the target object among four objects. *Top right:* The iTHOR agent navigates and finishes household tasks. *Lower left:* The Kuka moves its gripper tip to the target block among four identical blocks. *Lower right:* The deployment of a learned policy to a physical Kinova Gen3 and the fine-tuning of the policy in the real world.

corresponding target to finish the task given limited sensing. The end-to-end model in [5] directly maps sound commands and image observations to a sequence of robot actions that fulfill the commands, as illustrated in Fig. 2b. The model is first trained in a simulated environment using reinforcement learning (RL) and auxiliary losses, and then the model is deployed to a real robot without further training.

However, this model has its own weaknesses. First, the reward functions need to be hand-tuned and are task-specific, which limits the generalization of the method. Second, it is costly to improve the system after its deployment in a new domain. Ideally, when an intelligent voice-controlled robot encounters unseen scenarios, it should be able to continually improve its interpretation of language and skills from non-experts in daily life. However, improving the system requires prohibitive amount of labels to optimize auxiliary losses and accurate measurements to construct reward functions, both of which are difficult to obtain or not available from non-experts in the real world.

Based on recent advancements in representation learning, we address these weaknesses in [5] by proposing a two-stage pipeline for training RSI agents as shown in Fig. 2c. At the first stage, we train a visual-audio representation (VAR) whose training data can be collected easily and intuitively by non-experts. At the second stage, we use the VAR to produce an intrinsic reward function for RL training. The intrinsic reward function is general across tasks or robotic platforms, which avoids the laborious reward engineering. After the

P. Chang, S. Liu, and K. Driggs-Campbell are with the Department of Electrical and Computer Engineering at the University of Illinois at Urbana-Champaign. emails: {pchang17,sliu105,krdc}@illinois.edu

This work is supported by Agriculture and Food Research Initiative (AFRI) grant no. 2020-67021-32799/project accession no.1024178 from the USDA National Institute of Food and Agriculture.

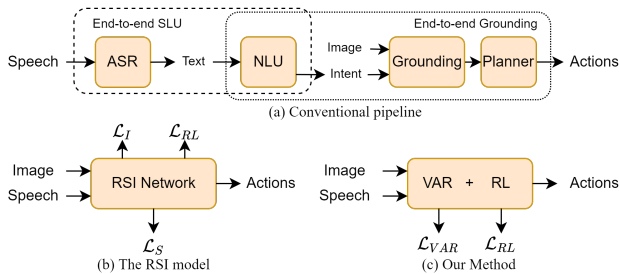


Fig. 2: **Illustration of different models for voice-controlled robots.** (a) A conventional pipeline for voice-controlled robots. Independent modules process the inputs. End-to-end SLU combines the ASR and the NLU, while end-to-end grounding combines the NLU and the grounding module. (b) The first RSI model [5]. Auxiliary losses such as \mathcal{L}_I and \mathcal{L}_S are used for classifying images and the intent in the speech, respectively. The model is trained end-to-end with an RL loss, \mathcal{L}_{RL} . (c) The proposed model.

robot is deployed in a new domain where an accurate reward is hard to obtain or not available, non-experts can easily fine-tune the VAR by providing a reasonable amount of training data, which updates intrinsic reward function and allows the robot to perform self-supervised skill improvement.

Our method is inspired by sensorimotor contingency which is the relations between an agent’s actions and the resulting sensory changes [6]. Imagine that an infant touches a bell by accident and hears a bell ring. Motivated by her “intrinsic curiosity,” she attempts to replicate the sound by repeating and refining the touching action [7]. When she hears a bell ring later, she should identify what actions are needed to ring the bell. We believe that a robot can associate the motor actions with the corresponding audio command through a similar learning process.

Our main contributions are as follows. (1) We present a novel pipeline for task-oriented voice-controlled robots inspired by sensorimotor theory. (2) We build a novel VAR that provides reward signals to the downstream RL training. The VAR can be treated as a unification of the ASR, NLU, and the grounding module. (3) Our system exhibits promising results in multiple navigation and manipulation tasks. We demonstrate that our new pipeline enables the robot to self-improve its policies with limited amount of data from a new domain using both simulated and real-world experiments. (4) We create and solve the first visually high-fidelity AI environment that uses real multi-word speech commands for instruction following tasks.

II. RELATED WORKS

A. Conventional voice-controlled robots

As shown in Fig. 2a, a conventional pipeline of voice-controlled robots usually consists of four independent modules: an ASR system to transcribe speech to text [8], an NLU system to map text transcripts to speaker intent [2], [9], a grounding module to associate the intent with physical entities [10], [11], and a planner to generate feasible trajectories for task execution [1], [12], [13]. However, the conventional pipeline is prone to intermediate errors. Off-the-shelf ASR systems usually operate in a general-purpose setting irrelevant to specific robotic tasks. Typical NLU systems, however, are trained on clean text [3]. As a result, the text

outputs could be inevitably out-of-context or erroneous [2], [14], which causes the overall task performance to degrade. Rule-based systems based on symbolic AI are used for grounding [15]. However, developing such system requires significant labor and these systems do not scale beyond their programmed domains [2], [4].

B. End-to-end language understanding and grounding

Different from the conventional ASR plus NLU pipeline, the end-to-end spoken language understanding (SLU) system maps the speech directly to the speaker’s intent without translating the speech to text [3], [16], [17]. The end-to-end learning avoids the intermediate errors and allows the models to fully exploit subtle information such as speaker emotion that are lost during transcription [16], [17]. Similar to a human, the end-to-end SLU system extracts high-level concepts in speech instead of understanding the speech by recognizing word by word [3]. However, end-to-end SLU systems are mainly used for virtual digital assistants and do not consider the complex grounding process in robotics.

End-to-end language grounding agents have been developed to perform tasks such as navigation [18], [19], object finding [4], [20], and household tasks [21] according to text-based natural language instructions and visual observations. Our work is different from them in several aspects. First, we focus on voice-controlled agents, while the above works consider text-based input which limits the potential of natural human-robot communication. Second, training these agents require either experts’ actions at every timestep or step-by-step instructions for imitation learning [18], [21] or a carefully designed extrinsic reward function for reinforcement learning [4], [19], [20]. In contrast, our method needs neither the expert demonstrations nor extrinsic reward functions, and thus requires less efforts to improve.

Studying how an embodied agent learns and builds its own interpretation of sound commands, RSI is the first work that combines the ideas from end-to-end SLU and language grounding agents for voice-controlled robots, where the ASR, the NLU, the grounding module, and the robot control are unified as an end-to-end model [5]. However, the method in [5] has limited ability to improve in different domains and generalize across different tasks and robots, as mentioned in Sec. I. In contrast, our work can be improved in a new domain and is general across tasks.

C. Representation learning for robotics

Representation learning has shown great potential in learning useful embeddings for downstream control tasks. Deep autoencoders are used to encode high-dimensional observations such as images into lower-dimensional vector embeddings. These vectors are then used as states or intrinsic reward functions for reinforcement learning [22], [23]. At test time, however, the methods in [22], [23] require users to provide goal images for task execution while we use voice control, which is a more natural and convenient way of human-robot communication. Additionally, reconstruction of the input images makes the autoencoders computationally

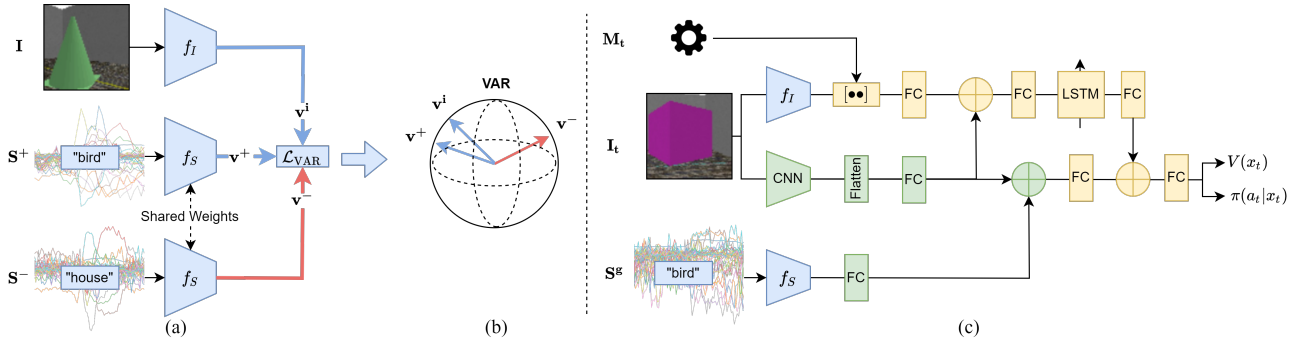


Fig. 3: **The network architectures.** (a) The VAR is a three-branch Siamese network optimized with triplet loss. (b) The latent space of the VAR is a unit hypersphere such that vector embeddings of images and audios of the same object are closer than those of different objects. (c) The policy network for RL training. The portion in blue is VAR and the weights are frozen in RL training. We use \oplus to denote element-wise addition, FC to denote fully connected layers, and $\bullet\bullet$ to denote concatenation.

expensive. Another line of work uses contrastive loss to learn representations for downstream tasks such as grasping and water pouring [24]–[26]. One advantage of using contrastive loss is that the loss avoids the reconstruction required by autoencoders. Different from all of these works that focus mainly on the visual or the text modality, we address the interplay between sight and sound.

III. METHODOLOGY

In this section, we describe our two-stage training pipeline and the fine-tuning procedure in a new domain. In training, we assume the availability of sufficiently large datasets and robotic simulators that can be used by professionals to develop and train the model. In fine-tuning, we assume that datasets, simulators, and professionals are not available.

A. Visual-audio representation learning

In the first stage of our pipeline, we learn a joint representation of images and audio, named VAR, that associates the image with the corresponding sound command. To mimic the sensorimotor learning experiences, the simulated environments for training the VAR act like children’s parents who tell the robot what it sees and does not see. For example, the environment provides triplet data to the robot, which is similar to a mother saying, “This is a cube, not a cone,” when her child is looking at a cube-shaped object. The agent is thus told whether an image is semantically similar or dissimilar to an audio, while the exact class of the image and the audio remains unknown to the agent.

1) *Simulation environment and data collection:* At each timestep, the environment produces a positive and a negative sound. If an object is in the view of the robot camera in a navigation task, or when the robot’s gripper tip aligns with an object in a manipulation task, the robot receives a positive sound command corresponding to the object and a negative sound command that does not match the object. We let the robot randomly move in the environment and automatically collect visual-audio triplets (I, S^+, S^-) , where $I \in \mathbb{R}^{n \times n}$ is the current RGB image from the robot’s camera and serves as the anchor, $S^+ \in \mathbb{R}^{l \times m}$ is the Mel Frequency Cepstral Coefficients (MFCC) [27] of the positive sound commands, and $S^- \in \mathbb{R}^{l \times m}$ is the MFCC of the negative sound commands. We use l to denote the number

of frames in time axis and m to denote the number of features in frequency axis. If the agent does not trigger a sound, the robot will hear no positive sound, $S^+ = \mathbf{0}_{l \times m}$. More specifically, in a manipulation task, the empty sound happens when its gripper tip is above none of the objects; in a navigation task, the empty sound happens when the robot does not see or is far away from all objects.

2) *Training the VAR:* Our goal is to encode both auditory and visual modalities into a joint latent space, where the embeddings of images and audios of the same intent are close together, and those of different intents are far apart. We formulate the problem as metric learning. As shown in Fig. 3a, the VAR is a Siamese network that has three branches for encoding the anchor image I , the positive sound S^+ , and the negative sound S^- . We use $f_S : \mathbb{R}^{l \times m} \rightarrow \mathbb{R}^d$ to encode both S^+ and S^- , where d is the dimension of the latent space, and we use $f_I : \mathbb{R}^{n \times n} \rightarrow \mathbb{R}^d$ to encode I . Then, $v^i = f_I(I)$, $v^+ = f_S(S^+)$, and $v^- = f_S(S^-)$ are the latent representation of I , S^+ , and S^- , respectively. We enforce the norm of v^i , v^+ , and v^- to be 1 by applying a $L2$ -normalization, such that the latent space lives on a unit hypersphere as shown in Fig. 3b. We use convolutional neural networks (CNN) and bidirectional recurrent neural network (BRNN) to process the sound signals, and we use CNN to process the images [28]–[30]. Practically, any deep models for sound and image processing can be used for f_S and f_I . We use triplet loss as the objective, which encourages the distance of vector embeddings between the anchor and the negative to be greater than that between the anchor and the positive by a margin of α [31]. The objective for optimizing f_I and f_S with a visual-audio triplet (I, S^+, S^-) is

$$\mathcal{L}_{VAR} = \max(0, \|v^i - v^+\|_2^2 - \|v^i - v^-\|_2^2 + \alpha) \quad (1)$$

B. RL with visual-audio representation

The second stage of our pipeline is to use RL to train the robot to reach goals using intrinsic reward functions generated by the trained VAR. We model this interaction as a Markov Decision Process (MDP), defined by the tuple $\langle \mathcal{X}, \mathcal{A}, P, R, \gamma \rangle$. At each time step t , the agent receives a current observation $x_t \in \mathcal{X}$ and takes an action $a_t \in \mathcal{A}$ based on its policy $\pi_\theta(a_t|x_t)$ parameterized by θ . In return, the agent receives an intrinsic reward r_t from VAR and

transitions to the next state x_{t+1} according to an unknown state transition $P(\cdot|x_t, a_t)$. The process continues until t exceeds the maximum episode length T and the next episode starts. The goal of the agent is to maximize the expected return, $R_t = \mathbb{E}[\sum_{i=t}^T \gamma^{i-t} r_i]$, where γ is a discount factor. The value function $V^\pi(x)$ is defined as the expected return starting from x , and successively following policy π .

1) *VAR-aided RL*: At each time step t , the agent receives an image \mathbf{I}_t from its camera, the MFCC of the current sound \mathbf{S}_t , and robot states \mathbf{M}_t such as end-effector location or odometry. The current sound \mathbf{S}_t is triggered in the same way as \mathbf{S}^+ in Sec. III-A.1. At $t = 0$, the agent receives an additional one-time sound command $\mathbf{S}^\mathfrak{g}$ corresponding to an intent. We define the state $x_t \in \mathcal{X}$ for the MDP to be $x_t = [\mathbf{I}_t, f_I(\mathbf{I}_t), f_S(\mathbf{S}^\mathfrak{g}), \mathbf{M}_t]$, where f_I and f_S come from the VAR which is fixed in this stage of the pipeline. The VAR compactly represents the high-dimensional observations and the intent contained in $\mathbf{S}^\mathfrak{g}$.

The VAR also generates intrinsic reward function which motivates the agent to reach the target. Suppose the embeddings of an image and a sound command of the same intent are close to each other in the VAR, the intrinsic reward function is the sum of two dot products

$$r_t = f_I(\mathbf{I}_t) \cdot f_S(\mathbf{S}^\mathfrak{g}) + f_S(\mathbf{S}_t) \cdot f_S(\mathbf{S}^\mathfrak{g}) \quad (2)$$

The first dot product $f_I(\mathbf{I}_t) \cdot f_S(\mathbf{S}^\mathfrak{g})$ measures the similarity between the current image and the sound command, while the second dot product $f_S(\mathbf{S}_t) \cdot f_S(\mathbf{S}^\mathfrak{g})$ is the similarity between the current sound and the sound command. Intuitively, the agent receives high reward when both the scene it sees and the current sound it hears match the sound command. Note that providing current sound signals to the system is optional and is feasible in the simulation. The current sound \mathbf{S}_t is not part of the state x_t and is only used to calculate the reward. Thus, the robot policy is not conditioned on \mathbf{S}_t and does not require sound feedback at test time. Chang *et al* use extrinsic reward functions that rely on task-specific or robot-specific ground-truth information from the simulator [5]. In contrast, our intrinsic reward function depends on the similarity of the embeddings and is thus agnostic to tasks and robots. Combining our intrinsic reward function with an extrinsic task-specific reward function is a design choice. Nevertheless, we show in Sec. IV that our model outperforms the baselines even with only the intrinsic reward.

2) *Network architecture*: Our policy network architecture is in Fig. 3c. The network takes x_t as input and output the value $V(x_t)$ and the policy $\pi(a_t|x_t)$. The reason that we need another CNN in the policy network is that f_I and the CNN may need to extract different features. For example, in a navigation task, the CNN needs to encode information about obstacles for collision avoidance, while f_I does not need to. The embeddings of image \mathbf{I}_t and robot state \mathbf{M}_t are fed into an LSTM for long-term decision making. But the goal sound $\mathbf{S}^\mathfrak{g}$ is not passed into an LSTM because it is an one-time signal. We use Proximal Policy Optimization (PPO) for policy and value function learning [32].

C. Fine-tuning

We assume that accurate speech transcriptions, one-hot labels, and tuned reward functions are not available during fine-tuning because they cannot be provided by non-experts. Since performing accurate measurements and data collection in the real world is expensive and hard, only scarce and noisy data from the non-experts are available. Our pipeline allows non-experts to intuitively fine-tune the model whose performance degrades due to domain shift after the deployment. Non-experts only need to provide triplets to the VAR as in Sec. III-A based on their common knowledge using their own voices. The non-experts do not need to know the total number of objects or the class index of each object. The collected triplets are used to fine-tune the VAR. We use $r_t = f_I(\mathbf{I}_t) \cdot f_S(\mathbf{S}^\mathfrak{g})$ as reward function if current sounds are not available. The agent can then perform self-supervised skill improvement with the intrinsic reward function from VAR. No additional labels or measurements other than the collected triplets are needed to support its RL training. If a user is able to provide current sounds, we can use Eq. 2 to perform real-time voice-based supervision to the robot.

IV. SIMULATION EXPERIMENTS

In this section, we first briefly describe the three robotic environments and sound data for the experiments. Then, we compare the performance and data efficiency of our pipeline with several baselines and ablation models.

A. Robotic Environments

We use three challenging simulation environments implemented using PyBullet and AI2-THOR in Fig. 1 to show that our model is general in terms of robotic platforms and tasks. The TurtleBot and the Kuka environments pose difficulties in fine motor control and have moderate difficulty for perception. The iTHOR environment is challenging in perception, while the control is discretized and simplified. In all environments, the monocular uncalibrated cameras only provide RGB images. No tags, depth, and models of the objects are given to the agent. The illustrations of the environments can be found in the Supplementary Video.

1) *TurtleBot*: The TurtleBot environment contains a 4m² arena and four objects: a cube, a sphere, a cone, and a cylinder. Each object is associated with an intent. The robot’s goal is to navigate to the object mentioned in a command based on RGB images. The agent needs to learn exploration skills to find the target object as quickly as possible.

2) *Kuka*: The Kuka environment contains a table and four identical blocks. Each block is associated with an intent. The robot’s goal is to move its gripper tip on the top of the block mentioned in a command based on images from a location-fixed camera. The agent needs to develop spatial reasoning skills to differentiate the target block from other identical blocks using the observed relative positional information.

3) *iTHOR*: Our iTHOR environment is the first AI environment with real multi-word speech commands. The environment consists of 30 different floor plans of living rooms and simulates real-world applications of household robots.

The intents include toggling on and toggling off the floor lamp and the television in a scene. The goal of the robot is to navigate to and manipulate the object mentioned in a sound command based on images and a noisy local occupancy map. The agent in the iTHOR environment needs to associate complex speech commands with rich visual observations and perform mapless navigation to finish the task.

B. Sound data processing

We consider various types of sounds including speech signals, environmental sounds, single-tone signals, and a mixture among them. For single-word speech signals, we choose “zero,” “one,” “two,” and “three” as Wordset1 from the Speech Commands Dataset [33]. For multi-word speech signals, we choose the speech with duration at most 6 seconds from the Fluent Speech Commands Dataset (FSC) [16]. FSC dataset is collected for contemporary end-to-end SLU system and contains commands used for a smart home or virtual assistant. The four intents we choose are “activate light,” “deactivate light,” “activate music,” “deactivate music.” For each intent, there are multiple possible wordings. For example, the intent of “activate light” can be expressed as “turn on the lights” and “lamp on.” For single-tone signals, we choose four musical notes, C_4 (Middle C), D_4 , E_4 , and F_4 , performed by various musical instruments from NSynth datasets [34]. We mix the sound data from two datasets to show that our model can map different types of sounds to one object or concept. In the Mix dataset, single-word speech signals are mixed with environmental sound coming from the UrbanSound8K Dataset [35]. For each intent, 1,000 samples are used for training and 50 samples are used for testing.

C. Experiment setup

We now introduce the training and evaluation of our pipeline in simulation. In our experiments, the overall architectures are kept the same for solving all the environments. Designing a specific network architecture for each individual task is not the focus of our paper. The sound commands for the iTHOR environment come from the FSC dataset, while the commands for the Kuka and the TurtleBot environments come from the other datasets.

1) *Training*: For all tasks, we first let the robot randomly explore the environment and collect 50,000 audio-visual triplets. The triplet margin $\alpha \in [1.0, 1.2]$ and the latent space dimension d is 3. During RL training, the VAR is fixed and 8 instances of the environment run in parallel.

2) *Evaluation criteria*: We test the trained policy for 50 episodes for each intent (200 episodes in total) with unheard sound data. For the Kuka environment, an episode is considered a success if the robot’s gripper stays close to the target block for more than 50 timesteps. For the TurtleBot environment, we define an episode as a success if the robot stays close to the target object for more than 5 timesteps. For the iTHOR environment, we define an episode as a success if the robot correctly toggles the floor lamp or television in a scene.

We evaluate the model with two metrics. The first metric is success rate, defined as the percentage of successful episodes in all test episodes. The second metric is label usage which includes one-hot labels and queries to the simulator. For example, measuring the distance between the robot and the goal is a query. One triplet requires two labels to indicate the positive and the negative.

3) *Baselines and Ablations*: We compare our method with three baselines and one ablation. The first baseline, denoted as “RSI 1,” is the method in [5] which has the access to hand-tuned task-specific reward functions and ground-truth class labels for the images and sounds. Every RSI 1 training step requires 3 labels, including 2 simulator queries to calculate the extrinsic reward and 1 one-hot label for auxiliary losses¹.

The second baseline, denoted as “NoAux+SparseR,” is a variant of RSI 1. We collect 50,000 one-hot labels to pretrain the network. During the RL training, we remove all the auxiliary losses, and we give the agent a reward of 1 if a task is completed and 0 otherwise at each timestep. This baseline shows the performance of “RSI 1” without ground-truth class labels and hand-tuned reward functions.

The third baseline, denoted as “ASR+NLU+RSI 1,” is a conventional pipeline². The speech is first transcribed by an off-the-shelf deep learning-based ASR named Mozilla DeepSpeech [30]. The output of the ASR is noisy. For example, “Play the music” is sometimes transcribed as “by the music.” We therefore train a learning-based NLU so that the correct intent can still be inferred given noisy inputs. The intent is then transformed into an one-hot encoding, which is fed to an RL agent whose architecture is the same as the RSI 1 except that sound processing network is removed.

The ablation model, denoted as “No current sound,” removes $f_S(\mathbf{S}_t) \cdot f_S(\mathbf{S}^g)$ from the intrinsic reward function, Eq. 2. The purpose of the ablation model is to quantify the effect of the current sound signal.

D. Results for control policies

1) *Unheard sounds*: In this experiment, all models are first trained with the same amount of RL steps without fine-tuning in each environment. Then, we test the models with sound commands that never appear during training. We use this experiment to compare the performance of the models when the amount of data and the training steps are sufficient. For the iTHOR environment, the total training steps is 6 million (M), and the agent is tested within the training floor plans (Floor Plan 201 - 220). The total training steps is 3M for both the Kuka and the TurtleBot environments.

From Table I and Table II, we find that our method generalizes well in terms of different types of sound commands and robotic tasks. Our method achieves 1% ~ 5% higher success rates compared with RSI 1 in all three environments,

¹The queries include target object state checking and distance measuring. For convenience purposes, we count the one-hot labels for all the auxiliary losses as one for RSI 1, which is lower than the real label counts.

²This pipeline is not used in the Kuka and the TurtleBot environment, because the sound commands in these environments involve non-speech content or only single words.

TABLE I: Testing results in the Kuka and the TurtleBot environments with different types of sounds.

Environment	Dataset	Success rate		
		NoAux+SparseR	RSI 1	Ours
Kuka	Wordset1	46.0	95.5	97.0
	NSynth	28.5	92.5	98.0
	Mix	23.0	94.0	95.5
TurtleBot	Wordset1	22.0	92.0	94.0
	NSynth	9.5	95.0	96.0
	Mix	21.0	87.0	91.0

TABLE II: Testing results in the iTHOR 201-220

Dataset	Models	Label usage	Success rate
FSC	NoAux+SparseR	6.0×10^6	26.0
	No current sound	0.1×10^6	61.5
	ASR+NLU+RSI 1	18.0×10^6	66.0
	RSI 1	18.0×10^6	68.0
	Ours	6.1×10^6	71.0

even though it has no access to ground-truth class labels or extrinsic reward functions during the whole RL training. We believe the reason is that RSI 1 optimizes multiple losses jointly, which may cause biased gradients. In contrast, our two-stage pipeline learns the two tasks separately, which benefits the training of both tasks. A common failure case for the iTHOR agent is that the agent is blocked by obstacles during its move to the correct target.

From Table I and Table II, the success rates for “NoAux+SparseR” baseline for all the environments are much lower than RSI 1 and our method. The result suggests that the performance of RSI 1 degrades significantly without unlimited ground-truth labels for its auxiliary losses and heavily hand-engineered reward function. In contrast, our method can perform better even with weaker supervision and fewer engineering efforts and is thus more general.

From Table II, The success rate for “ASR+NLU+RSI 1” baseline is lower than both the RSI 1 and our method. As mentioned in Sec. II-A, the pipeline is prone to intermediate errors and thus has lower success rate. This result justifies the usage of end-to-end SLU in RSI 1 and our work.

The success rate for “No current sound” ablation is only 9.5% lower than our method, but the label usage of this ablation is significantly lower than all other models. The result indicates that our method works reasonably well without the current sound signals that can be hard to obtain in the real world and providing current sound signals further increases the performance.

2) *Unseen scenes*: We test the performance of our method and the RSI 1 with unheard sound commands in unseen floor plans in the iTHOR environment. Different from the experiment in Sec. IV-D.1, where the models are trained without constraints on label usages, this experiment simulates the fine-tuning in the real world and quantifies the label efficiency of the models. Each model is given the same amount of labels, and a high-efficiency model should achieve higher success rate compared to a low-efficiency model.

We use “0” to denote the direct deployment of the models without further training in any unseen floor plans. We use “5000” to denote the settings where a total amount of 5000 labels are collected and are used for the fine-tuning. We follow the fine-tuning procedure mentioned in Sec. III-C without providing the current sound signals. We train another RSI 1 model for 1M steps, which uses about 3M labels as an oracle model to approximate the highest possible success rates. The results are shown in Table III.

TABLE III: Success rates of different methods after fine-tuning in unseen Floor Plan 226 - 230 with FSC dataset.

Labels	0		5000			3M	
	RSI 1	Ours	RSI 1	Ours 0.08M	Ours 0.4M	Ours 1M	RSI 1
Avg.	30.7	31.5	37.2	67.5	73.7	84.7	90.8

From Table III, we find that the RSI 1 baseline can only be improved by 6.5% using 5000 labels, while our method improves itself by 36%, 42%, and 53% after 0.08M, 0.4M, and 1M RL training steps, respectively, using the same amount of labels. We also see that the average gap between Ours 1M and the oracle is only 6%, suggesting that our model achieves high performance using limited amount of labels. In the fine-tuning stage, RSI 1 uses the labels for policy network fine-tuning, which leads to fast depletion of the label quotas and less RL experience, which suggests that fine-tuning the RSI 1 is unrealistic. The richer RL experience in our method is due to its higher efficiency because labels are used to predict the intrinsic reward and there is no label consumption during its self-supervised RL exploration. We believe that this result is satisfying given that the current sound is not provided and that the amount of label usage is 600 times less than that of the oracle model.

TABLE IV: Model performance and the number of triplets collected for the fine tuning

Floor Plan	RL Training Steps	Number of Triplets		
		<500	1000	2500
226	0.08M	59.0	79.0	83.5
	0.4M	75.0	84.5	88.0
	1M	86.5	91.0	92.5
230	0.08M	49.0	45.0	45.0
	0.4M	62.0	63.0	57.0
	1M	77.0	80.5	86.5

3) *Performance and the number of triplets*: We explore the relation between the model performance during the fine-tuning and the number of triplets in two randomly picked floor plans. From Table IV, we see that the more triplets are provided, the better the final performance becomes. This observation is reasonable since more training data leads to better VAR and reward functions. We find that the performance is reasonably well even if the amount of triplets provided are less than 500, which suggests that the VAR has high data efficiency.

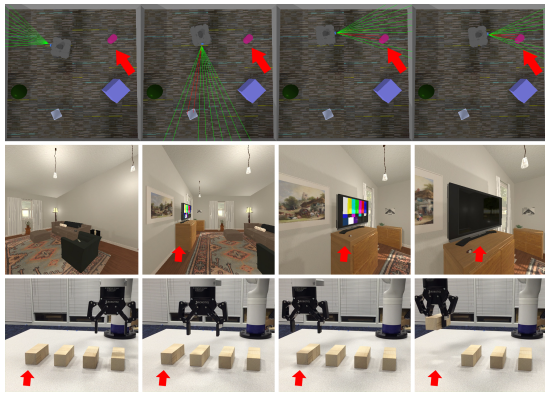


Fig. 4: **Qualitative Result in the simulation and the real world.** The target objects are indicated by the red arrows. Green and red lines are invisible to the robots. *Top*: Simulated TurtleBot searches and approaches its target, the purple cylinder. *Middle*: iTHOR agent searches for the television and turn it off. *Bottom*: The real Kinova Gen3 moves its gripper to the target block and performs a successful grasp.

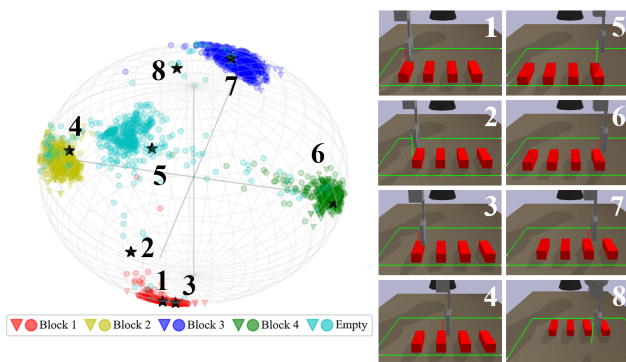


Fig. 5: **Visualizations of the VAR in the Kuka environments with Wordset1.** The colors indicate the ground truth labels of sound and image data. In the sphere, the embeddings of images are marked by circles and sounds are marked by triangles. The black stars are the vector embeddings of the 8 images. Block 1 is the leftmost block. The “Empty” class consists of empty sounds and images of the gripper tip above none of the blocks.

4) *Qualitative results*: Fig. 4 and the attached video show examples of the agent successfully reaching their goals.

E. Qualitative results of the VAR

To better understand the VAR and how it produces an effective intrinsic reward, we plot the vector embeddings of some positive pairs from the audio-visual triplets with the trained VAR in Fig. 5. In the VARs of all three environments, the embeddings of images and sounds of the same concept form a cluster and all clusters are separated from each other. Thus, the agents successfully associate images and sounds with the same meanings and distinguish those with different meanings, even though we do not explicitly classify the objects or inform the agent of the number of classes.

We also find that the VAR is able to map the images with ambiguous labels to meaningful locations on the spheres. For example, in Fig. 5, the gripper tip in #2 is not directly above but is very close to Block 1. In the VAR sphere, the vector embedding is indeed between the Block 1 (red) and the Empty (cyan) cluster. With the ability to represent ambiguous images, the VAR generates a relatively dense reward function that guides the robot exploration in RL. In the same example, suppose Block 1 is the target block, the reward in Eq. 2 are

higher in #2 than those in #4 or #5. Thus, the reward is higher when the gripper is around the target block and lower when the gripper is far away from the target.

V. REAL-WORLD EXPERIMENTS

To show the effectiveness of our method on real physical robots and its potential to improve itself in the real world, we use a Kinova Gen3 arm for the Kuka choosing task, train the robot in the simulator and fine-tune the model in the real world. We assign the four blocks from left to right with the words “zero,” “one,” “two,” and “three.” At every timestep, the trained agent receives an image from an uncalibrated location-fixed RGB camera and its end-effector location in the workspace. All sound commands for testing are unheard during training. The trained model controls the robot gripper to move towards the target block and adjusts its pre-grasp pose. At the end of an episode, the robot lowers its gripper vertically and perform a grasp on the chosen block.

We use domain randomization to learn robust features in both stages of our pipeline. We randomize the color and texture of the blocks and the background during training. We also randomize the camera viewpoint and the relative positions among the blocks.

Results with domain randomization: We first deploy the model trained with domain randomization to a real Kinova Gen3 without real-world fine-tuning and count the number of successful grasps. In the first row of Table V, the results indicate that the simulation to real world transfer is successful in some cases. We believe the failures are caused by the difference in camera pose between the simulation and the real world. The result suggests that the domain randomization only helps bridge the sim2real gap to some extent, and thus this technique alone can be insufficient for real-world learning-based robotic applications.

TABLE V: Success counts for each intent and average success rate with a total of 48 tests (12 for each intent)

Words	“zero”	“one”	“two”	“three”	avg.
Domain randomization	8	11	9	7	72.9
Fine-tuning	11	9	11	12	89.6

Results with fine-tuning: We show that our method can self-improve in the real world by fine-tuning the model with real world data. Specifically, in the real world environment, we spend about 1 hour in manually collecting 993 triplets, which are used to fine-tune the VAR and the RL policy. No additional labels or supervision are needed from the humans since the intrinsic rewards are calculated by VAR. We train the model with randomized block positions for 10000 steps, which costs about 1 hour. In Table V, the average performance after fine-tuning increases 16.7% compared with domain randomization, which is significant given the relatively small number of real-world data and training time. In the failure cases, the agent is able to move towards the correct block, but only fails at grasping because the block is not completely within its jaw. A typical successful episode is shown in Fig. 4.

VI. CONCLUSION AND FUTURE WORK

We propose a general and self-improvable pipeline for vision-based voice-controlled robots. In our pipeline, we first learn a VAR, which associates images and sounds of the same concept. Then, we use the representation to generate an intrinsic reward function and embeddings for the downstream control tasks. Our method requires fewer labels yet outperforms baselines that has access to extrinsic reward functions across various types of sounds and robotic tasks in simulation. We also successfully transfer the policy to a real robot and improve the policy with small amounts of data in the real world. Possible directions for the future work include: (1) generalizing the same VAR to different downstream tasks, and (2) learning the representation in a self-supervised way without labeled triplets.

REFERENCES

- [1] R. Liu and X. Zhang, "A review of methodologies for natural-language-facilitated human-robot cooperation," *International Journal of Advanced Robotic Systems*, vol. 16, no. 3, 2019.
- [2] Y. Tada, Y. Hagiwara, H. Tanaka, and T. Taniguchi, "Robust understanding of robot-directed speech commands using sequence to sequence with noise injection," *Frontiers in Robotics and AI*, vol. 6, p. 144, 2020.
- [3] D. Serdyuk, Y. Wang, C. Fuegen, A. Kumar, B. Liu, and Y. Bengio, "Towards end-to-end spoken language understanding," in *International Conference on Acoustics, Speech, and Signal Processing (ICASSP)*. IEEE, 2018, pp. 5754–5758.
- [4] K. M. Hermann, F. Hill, S. Green, F. Wang, R. Faulkner, H. Soyer, D. Szepesvari, W. M. Czarnecki, M. Jaderberg, D. Teplyashin, et al., "Grounded language learning in a simulated 3d world," *arXiv preprint arXiv:1706.06551*, 2017.
- [5] P. Chang, S. Liu, H. Chen, and K. Driggs-Campbell, "Robot sound interpretation: Combining sight and sound in learning-based control," in *IEEE/RSJ International Conference on Intelligent Robots and Systems (IROS)*. IEEE, 2020, pp. 5580–5587.
- [6] J. K. O'Regan, *Why red doesn't sound like a bell: Understanding the feel of consciousness*. Oxford University Press, 2011.
- [7] L. Jacquey, G. Baldassarre, V. G. Santucci, and J. K. O'regan, "Sensorimotor contingencies as a key drive of development: from babies to robots," *Frontiers in neurobotics*, vol. 13, p. 98, 2019.
- [8] R. A. S. Fernandez, J. L. Sanchez-Lopez, C. Sampedro, H. Bavlle, M. Molina, and P. Campoy, "Natural user interfaces for human-drone multi-modal interaction," in *IEEE International Conference on Unmanned Aircraft Systems (ICUAS)*, 2016, pp. 1013–1022.
- [9] E. Bastianelli, D. Croce, A. Vanzo, R. Basili, and D. Nardi, "A discriminative approach to grounded spoken language understanding in interactive robotics," in *International Joint Conference on Artificial Intelligence (IJCAI)*, 2016, pp. 2747–2753.
- [10] R. Paul, J. Arkin, D. Aksaroff, U. Roy, and T. M. Howard, "Efficient grounding of abstract spatial concepts for natural language interaction with robot platforms," *The International Journal of Robotics Research*, vol. 37, no. 10, pp. 1269–1299, 2018.
- [11] A. Magassouba, K. Sugiura, A. T. Quoc, and H. Kawai, "Understanding natural language instructions for fetching daily objects using gan-based multimodal target-source classification," *IEEE Robotics and Automation Letters*, vol. 4, no. 4, pp. 3884–3891, 2019.
- [12] F. Stramandinoli, V. Tikhonoff, U. Pattacini, and F. Nori, "Grounding speech utterances in robotics affordances: An embodied statistical language model," in *Joint IEEE International Conference on Development and Learning and Epigenetic Robotics (ICDL-EpiRob)*, 2016, pp. 79–86.
- [13] H. Chen, H. Tan, A. Kuntz, M. Bansal, and R. Alterovitz, "Enabling robots to understand incomplete natural language instructions using commonsense reasoning," in *IEEE International Conference on Robotics and Automation (ICRA)*. IEEE, 2020, pp. 1963–1969.
- [14] A. Vanzo, D. Croce, E. Bastianelli, R. Basili, and D. Nardi, "Robust spoken language understanding for house service robots," *Polibits*, no. 54, pp. 11–16, 2016.
- [15] J. Savage, D. A. Rosenblueth, M. Matamoros, M. Negrete, L. Contreras, J. Cruz, R. Martell, H. Estrada, and H. Okada, "Semantic reasoning in service robots using expert systems," *Robotics and Autonomous Systems*, vol. 114, pp. 77–92, 2019.
- [16] L. Lugosch, M. Ravanelli, P. Ignoto, V. S. Tomar, and Y. Bengio, "Speech model pre-training for end-to-end spoken language understanding," in *Annual Conference of the International Speech Communication Association (INTERSPEECH)*, 2019.
- [17] M. Kim, G. Kim, S.-W. Lee, and J.-W. Ha, "St-bert: Cross-modal language model pre-training for end-to-end spoken language understanding," in *International Conference on Acoustics, Speech, and Signal Processing (ICASSP)*. IEEE, 2021, pp. 7478–7482.
- [18] P. Anderson, Q. Wu, D. Teney, J. Bruce, M. Johnson, N. Sünderhauf, I. Reid, S. Gould, and A. van den Hengel, "Vision-and-language navigation: Interpreting visually-grounded navigation instructions in real environments," in *IEEE Computer Society Conference on Computer Vision and Pattern Recognition (CVPR)*, 2018, pp. 3674–3683.
- [19] H. Yu, H. Zhang, and W. Xu, "Interactive grounded language acquisition and generalization in a 2d world," in *International Conference on Learning Representations (ICLR)*, 2018.
- [20] D. S. Chaplot, K. M. Sathyendra, R. K. Pasumarthi, D. Rajagopal, and R. Salakhutdinov, "Gated-attention architectures for task-oriented language grounding," in *Conference on Artificial Intelligence (AAAI)*, 2018, pp. 2819–2826.
- [21] M. Shridhar, J. Thomason, D. Gordon, Y. Bisk, W. Han, R. Mottaghi, L. Zettlemoyer, and D. Fox, "Alfred: A benchmark for interpreting grounded instructions for everyday tasks," in *IEEE Computer Society Conference on Computer Vision and Pattern Recognition (CVPR)*, June 2020.
- [22] A. Nair, V. Pong, M. Dalal, S. Bahl, S. Lin, and S. Levine, "Visual reinforcement learning with imagined goals," in *Advances in Neural Information Processing Systems (NeurIPS)*, vol. 31, 2018.
- [23] Y. Wang, G. N. Narasimhan, X. Lin, B. Okorn, and D. Held, "Roll: Visual self-supervised reinforcement learning with object reasoning," in *Conference on Robot Learning (CoRL)*, 2020.
- [24] P. Sermanet, C. Lynch, Y. Chebotar, J. Hsu, E. Jang, S. Schaal, S. Levine, and G. Brain, "Time-contrastive networks: Self-supervised learning from video," in *IEEE International Conference on Robotics and Automation (ICRA)*. IEEE, 2018, pp. 1134–1141.
- [25] E. Jang, C. Devin, V. Vanhoucke, and S. Levine, "Grasp2vec: Learning object representations from self-supervised grasping," in *Conference on Robot Learning (CoRL)*, 2018.
- [26] T. Nguyen, N. Gopalan, R. Patel, M. Corsaro, E. Pavlick, and S. Tellex, "Robot Object Retrieval with Contextual Natural Language Queries," in *Proceedings of Robotics: Science and Systems*, 2020.
- [27] S. Davis and P. Mermelstein, "Comparison of parametric representations for monosyllabic word recognition in continuously spoken sentences," *IEEE transactions on acoustics, speech, and signal processing*, vol. 28, no. 4, pp. 357–366, 1980.
- [28] D. Harwath, A. Torralba, and J. R. Glass, "Unsupervised learning of spoken language with visual context," in *Advances in Neural Information Processing Systems (NeurIPS)*, 2017.
- [29] K. Simonyan and A. Zisserman, "Very deep convolutional networks for large-scale image recognition," in *International Conference on Learning Representations (ICLR)*, 2015.
- [30] A. Hannun, C. Case, J. Casper, B. Catanzaro, G. Diamos, E. Elsen, R. Prenger, S. Satheesh, S. Sengupta, A. Coates, et al., "Deep speech: Scaling up end-to-end speech recognition," *arXiv preprint arXiv:1412.5567*, 2014.
- [31] F. Schroff, D. Kalenichenko, and J. Philbin, "Facenet: A unified embedding for face recognition and clustering," in *IEEE Computer Society Conference on Computer Vision and Pattern Recognition (CVPR)*, 2015, pp. 815–823.
- [32] J. Schulman, F. Wolski, P. Dhariwal, A. Radford, and O. Klimov, "Proximal policy optimization algorithms," *arXiv preprint arXiv:1707.06347*, 2017.
- [33] P. Warden, "Speech commands: A dataset for limited-vocabulary speech recognition," *arXiv preprint arXiv:1804.03209*, 2018.
- [34] J. Engel, C. Resnick, A. Roberts, S. Dieleman, D. Eck, K. Simonyan, and M. Norouzi, "Neural audio synthesis of musical notes with wavenet autoencoders," in *International Conference on Machine Learning (ICML)*, 2017, pp. 1068–1077.
- [35] J. Salamon, C. Jacoby, and J. P. Bello, "A dataset and taxonomy for urban sound research," in *International Conference on Multimedia (ACM-MM)*, Orlando, FL, USA, Nov. 2014, pp. 1041–1044.